

A SPHERICAL TEST ARTIFACT TO EVALUATE THREE-DIMENSIONAL FORM ACCURACY FOR WIRE ARC ADDITIVE MANUFACTURING

S. Ko*†, T. Sagawa*, Y. Yamagata*, S. Aoki*, and T. Abe**

*Institute of Technology, Shimizu Corporation, Japan

†Corresponding author, E-mail: s_ko@shimz.co.jp

**Division of Mechanical Engineering and Science, Saitama University, Japan

Abstract

Additive manufacturing, including the wire arc additive manufacturing (WAAM), is gradually gaining attraction, and providing benefits in the aerospace and construction industries. In both industries, large-scale manufacturing capability and quality consistency of manufactured 3D parts are crucial. As part of quality evaluation, test artifacts for the geometric capability assessment are specified in ISO/ASTM52902-2019(E). On the other hand, the test artifact for curved wall is left undefined. This paper proposes a spherical shell shape as a representative of three-dimensional shapes that are supportless and feature large overhangs, for testing the geometric capability of a WAAM equipment. A mechanical configuration and deposition strategy are considered, which owns the potential to universally applying for depositing large-scale parts. A quality evaluation process for the sphere deposition was also described and experimentally demonstrated.

Keywords: Wire arc additive manufacturing (WAAM), Test artifact, Inspection process, Sphere

Introduction

The combination of an electric arc as heat source and wire as feedstock is referred as Wire Arc Additive Manufacturing (WAAM) [1, 2]. The combined use of multi-axis robot systems and wire arc additive manufacturing (WAAM) offers tremendous advantages in the flexibility and the large-scale manufacturing capability [3]. The same with other metal AM technologies, WAAM can save manufacturing lead time [3], reduce the waste, therefore lower the environment impact [4,5]. WAAM process can also meet the emerging flexibility requirements, such as integrated printing of complex shapes through functional optimization [5]. Thanks to the wire feed stock, the deposition rate of the WAAM process is basically 4 to 9 times compared to other AM technologies using powder by referring [5]. Generally, metal AM faces a limited surface finish level which deeply depends on the particle size of the powder or the diameter of the wire. Therefore, one of the typical applications of a DED (Directed energy deposition) technologies (including WAAM) is for the production that can accept a near net shape surface finish or with a subsequent machining process [6]. Although the discussion on the geometric accuracy of the wire arc additive manufactured parts could be found in [5, 16], the standardization on the evaluation and the assessment of the geometric errors by the WAAM process remains limited in the literature.

For the additive manufacturing area, test artifacts for the geometric capability are proposed in ISO /ASTM52902-2019(E) [7]. However, only simple shapes such as hole, cylinder, slot, and straight walls are included. With the combination of the typical shapes, it is easy to access and possible to evaluate the basic geometric capability of the equipment. On the other hand, curved

wall, which is defined as a three-dimensional shell with different cross section in deposition direction [8] is difficult to be evaluated by ISO /ASTM52902-2019(E) [7]. Curved wall with large overhang feature can be deposited without printing extra support structures, by changing the direction of material accumulation during the fabrication process [3, 5], which is seen as a big advantage of WAAM process compared to other metal AM such as powder bed fusion (PBF) or direct energy deposition (DED) using metallic powder [8~11]. Therefore, the evaluation of the curved wall geometric capability is important for WAAM equipment.

To standardize the evaluation of the curved wall geometric capability, especially targeting to large scale workpieces, a sphere shape wall as a representative of three-dimensional shapes that are supportless and feature large overhangs, is proposed. A mechanical configuration and deposition strategy are considered, which owns the potential to universally applying for depositing large scale parts. A quality evaluation process for the sphere deposition was also described and experimentally demonstrated.

A spherical test artifact for curved wall deposition evaluation

WAAM is suitable for medium to large scale parts with low to medium geometric complexity [5]. The authors categorize the features available with WAAM process by the geometric complexity into Table 1. In which, the detailed feature of the Profile - Step 3 (multiple branches) can refer to [12]. The detailed feature of the Internal structure - Step 3 (lattice) can refer to [4, 13]. A spherical shell is a typical 3D shape that fully demonstrate the advantage of WAAM technology. In this study, the spherical shell is selected as the test artifact to evaluate the geometric accessibility of the WAAM equipment. Notice that, the deposition of multiple branches is more related to the path planning strategy, which is basically deployed by software development. The authors consider that the evaluation of sphere deposition can partially represent the multiple branches as well. On the other hand, lattice structure is not in the evaluation range of the proposed spherical test artifact. Considering that the strong point of WAAM process is in the large-scale parts with geometric complexity up to medium level, lattice structure (high geometric complexity) with WAAM process is still far away from standardization and needs further research effort for the deposition feasibility and process stability control.

Table 1 Available deposition objects with WAAM process

| | |
|--------------------|---|
| Profile | Step 1: 2.5D shape |
| | Step 2: 3D shape with single branch |
| | Step 3: 3D shape with multiple branches |
| Internal structure | Step 1: Shell model |
| | Step 2: Solid object |
| | Step 3: Lattice structure |

By clarify the deposition strategy and geometric evaluation of the spherical test artifact with WAAM process, it would contribute to fabricate most of the target parts with curved wall feature.

Strategy to deposit a large-overhang and support-free 3D shape

For large-overhang objects deposition, extra support structure is usually necessary. Some application with power-bed fusion [14] could deposit wall with a 10° tilt angle from the horizontal plane. While for WAAM, or the traditional welding process, 30° would be the limitation from our experience if we set the torch to be perpendicular to the horizontal plane. To overcome this limitation, a tilting rotary table with a swiveling axis was used to change the pose of the target part in [9, 10]. However, deposition of the parts in meters scale, which is generally used in the construction and the aerospace industries, would be difficult if the tilting of the deposited part becomes necessary, since of the gravity effect. A rigid fixture and safety measures becomes necessary to tilt the meter scale part and consequently the production becomes high-priced. Therefore, we propose a deposition strategy that basically always keep the deposited part in the horizontal plane. The raw material, which is the wire (and the torch) is kept in the tangential direction with respect to the deposited base. As well, the configuration to fit the deposition strategy, is also considered. Notice that Relativity Space [11] accepted similar deposition strategy in the Stargate Series 3D printers, while limited research results are published in the academia.

Curved wall [8], as described previously, is defined as a three-dimensional shell with different cross section in deposition direction. **Fig. 1** shows the conceptual scheme of the deposition strategy for the curved wall. In **Fig. 1**, the center, and the rotation with an angular speed ω around Z-axis can be defined. The slicing surface will slice the 3D model layer by layer in the Z-direction. The pose of the tool (a torch shown in **Fig. 1**) will be in a tangential direction from previous layer to the depositing layer. The distance between these two layers (called layer thickness) is setup to be in the tangential direction of the contour. Since the wire feed speed [15] in a WAAM process is set to be constant basically, the angular speed ω (rad/min) need to be specified following linear travel speed (mm/min) $F = R \omega$. In which, R (mm) represents the distance between the contour and the Z-axis, as shown in **Fig. 1**.

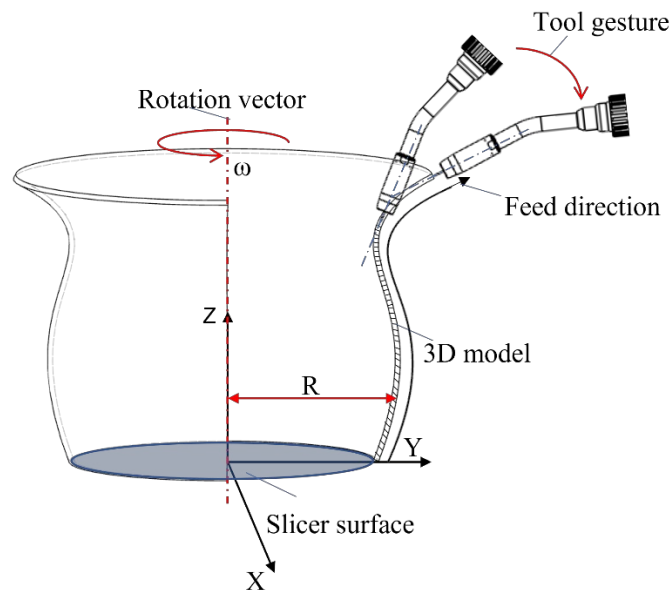


Fig. 1. Conceptual scheme to deposit curved wall

A schematic design of the WAAM equipment fit for the meters-scale parts commonly used in the construction and the aerospace industries, is illustrated in **Fig. 2**. It includes a 6-DOF (degree of freedom) industrial robot with a welding torch as the end effector, and a rotary table that rotates around Z-axis in horizontal plane. A metal wire will be feeding from the center of the torch during the WAAM process, depositing layers of metal on top of each other to a desired 3D shape. The motion generated by the slicing algorithm, will be transformed to the rotation of the rotary table and the motion of the industrial robot. The pose of the welding torch should be tilted in YZ-plane (around X-axis), to keep the torch in the tangential direction relative to the deposited part. Consequently, the translational movement of the industrial robot can be limited to the minimum in this configuration. The configuration can provide an excellent deposition envelope with a limited robot size. By limiting the motion of the 6-DOF industrial robot, the influence of the volumetric errors by the robot, can be limited to minimum [17]. Moreover, it fits better to the deposition of a meters-scale part with large-overhang, compared to the process mentioned in [9], since it is basically impossible to swiveling the parts considering the height of the parts.

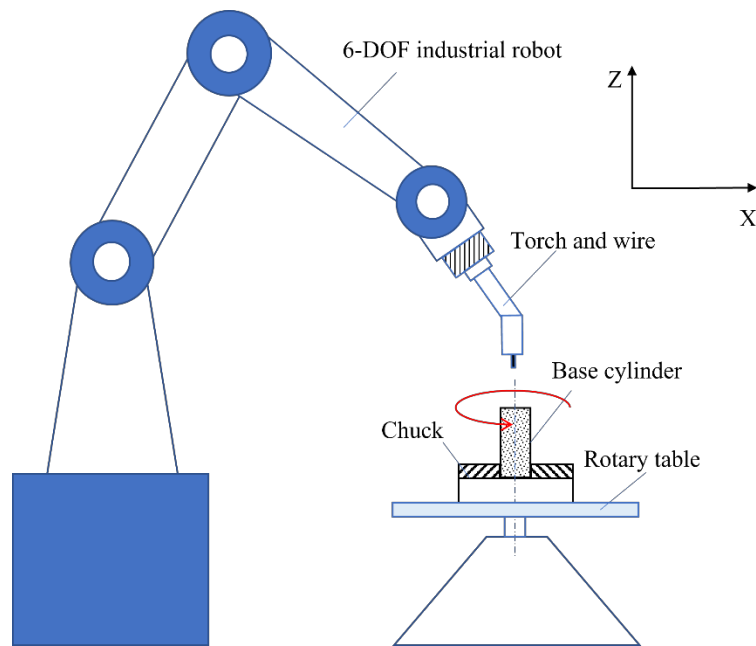


Fig. 2. The configuration of the WAAM equipment with a 6-DOF industrial robot and a rotary table

Table 2 The Experimental configuration of the WAAM equipment

| | |
|-------------------|------------------------|
| Industrial robot: | Yaskawa AR1440/YRC1000 |
| Rotary table: | Yaskawa MOTOPOS-D250F |
| Welding power: | Fronius TPS400i |
| Torch: | Fronius MTB400i 22° |
| Fixture (chuck): | NOBEL WP-300 |

To verify the feasibility of the considered deposition strategy, a sphere with a radius of 100mm was printed. The equipment used is listed in **Table 2**. The deposition conditions are shown in

Table 3. The deposited sphere is shown in **Fig. 3(a)**. Notice that Yaskawa MOTOPOS-D250F consists of one swiveling axis around X-direction and one rotary axis around Z-direction. In the sphere deposition process, the swiveling axis was not used and was kept in 0° to make the top of the rotary table in the horizontal plane.

As the base for the sphere deposition, a base cylinder with a diameter of 60 mm, was clamped by a manual screw chuck and aligned to the center of the rotary table. The deposition of the sphere started from the outer diameter of the base cylinder (60 mm) and ended in the diameter of 60 mm before the peak of the sphere, to prevent interference between the torch and the deposited part.

Table 3 Deposition conditions

| Parameter | Value |
|----------------------------|---------------|
| Base cylinder (A5052(JIS)) | D60mm H150mm |
| Wire material | A5356-WY(JIS) |
| Wire diameter | 1.2 mm |
| Wire feed speed | 2.9 m/min |
| Current | 41 A |
| Voltage | 11.1 V |
| Travel speed | 600 mm/min |
| Deposition rate | 0.5 kg/h |
| Target height per layer | 1.95mm |
| Environment Temperature | 24°C |

Inspection process and case study to evaluate the quality of the deposited 3D shape

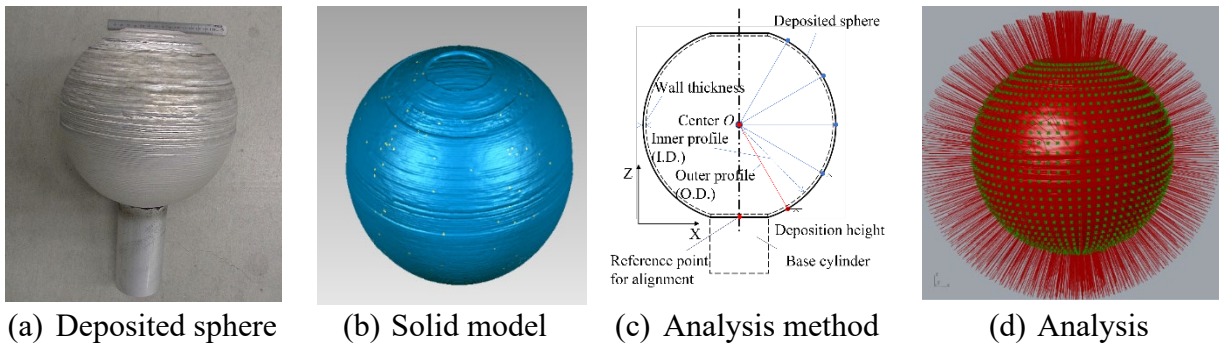


Fig. 3. The profile analysis of the solid model generated by CT scanning

Table 4 Suggested measurement parameters for spherical test artifact

| Parameters | Command | Measured by CT Scanning |
|---|------------|---------------------------|
| Inner sphere radius ($R_i \pm 1\sigma$) | 97.425 mm | 97.431 mm \pm 1.561 mm |
| Outer sphere radius ($R_o \pm 1\sigma$) | 100.425 mm | 102.274 mm \pm 1.287 mm |
| Wall thickness ($t \pm 1\sigma$) | 3 mm | 4.9 mm \pm 0.6 mm |
| Void volume ratio | - | 0.005% |

The deposited parts need to confront the weaknesses that is typically exist in the WAAM process, such as the integrity (the state of being fully dense), and the geometric accuracy [5, 15, 16]. Nevertheless, the deposition strategy considered here could have some concern on the integrity, referring to the traditional welding process [18]. Therefore, a scanning on the deposited part by using X ray computed tomography equipment (CT Scanner) was chosen in this study, since it has the advantage of non-destructively inspecting the porosity and the geometric accuracy [19].

Here below, an analysis process on the deposited sphere by using CT Scanning, is introduced. The analysis process includes three characterizations, 1) void volume analysis; 2) profile analysis; and 3) wall thickness analysis. As pointed out in [2], thermal influence is crucial in WAAM process. The heat accumulates and the profile of the weld bead can be varied as the deposition progresses [2]. Therefore, the characterizations depending on the deposition height, are of the authors' interest. Since they can provide the information necessary to improve the large-scale deposition process.

The experiment was conducted on a CT Scanner (XT H225ST by Nikon Solutions) [20]. VGSTUDIO (by Volume Graphics) [21] is used for the CT data analysis. The 3D model generated by the CT Scanning are shown in **Fig. 3(b)**. Especially for the 2) profile analysis and 3) wall thickness analysis, an analysis method on the 3D model generated by the CT Scanning is considered, as shown in **Fig. 3(c-d)**.

The definition of the analysis is shown in Fig.3 (c). The reference point to align the 3D model of the deposited sphere with the designed sphere, is setup to be the starting layer on the base cylinder (diameter 60 mm). The center of the sphere O is calculated based on the measured radius of the sphere. The radius of the outer profile and the radius of the inner profile can be calculated. They are summarized depending on the deposition height (see **Fig. 3(c)**). By calculating the distance between these two sets of data, the wall thickness depending on the deposition height can be calculated. Notice that a software named Geomagic Wrap [22] is used to repair the solid model generated by CT Scanning. After that, the calculation algorithm is implemented under Rhinoceros and Grasshopper.

The suggested measurement parameters for the spherical test artifact are listed up in **Table 4**. The measurement results by CT Scanning are shown as well.

1. Void volume analysis

The void can be detected and visualized, by the Porosity/Inclusion Analysis Module in VGSTUDIO [21]. The void volume, depending on the deposition height, is illustrated in **Fig. 4**. It shows that, only some dozens of voids within 0.1 mm^3 were detected, although there are multiple voids of 6 mm^3 max, especially in the deposition height 0 mm. The reason could come from a special pulse welding setting used only in the first layer to get a better penetration. the void volume ratio is 0.005% even including the deposition height 0 mm, which is considered not critical for this case study. We can conclude that the change of the torch pose doesn't affect the porosity of the

curved wall. Remark that the voids occurred at deposition height 195 mm, which could be the influence from the cumulative error between the robot trajectory and the deposited part.

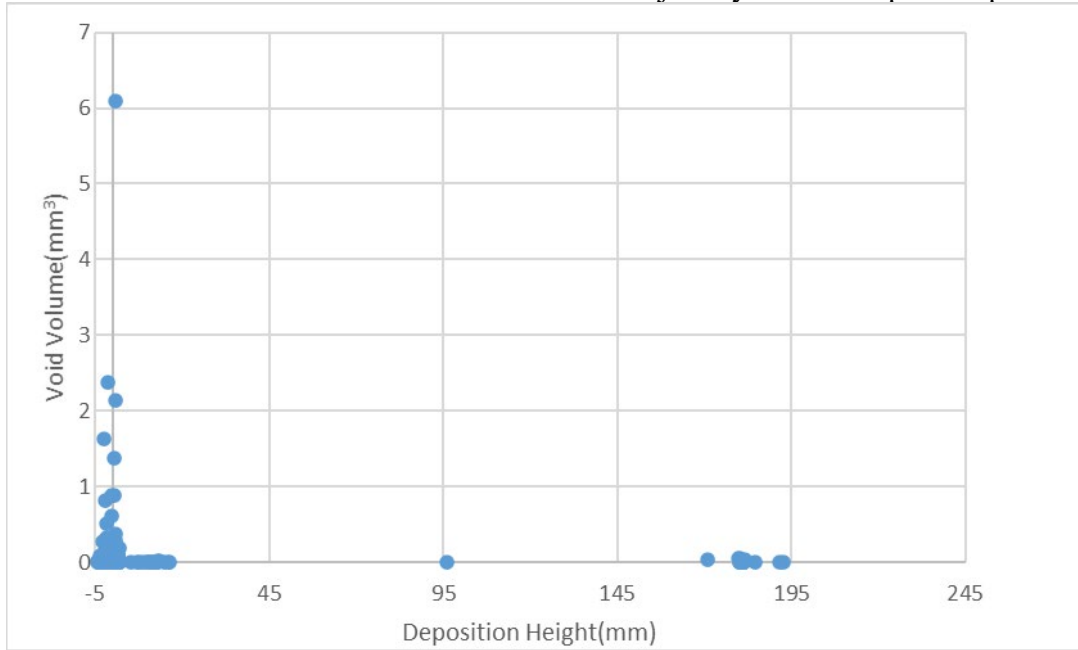


Fig. 4. The void volume analysis of the solid model generated by CT scanning

2. Profile analysis

The cross section of the deposited sphere in XZ plane measured by CT scanning, is shown in **Fig.5**. The profile and the wall thickness can be observed and discussed qualitatively. To further analyze the profile, the analysis described in **Fig. 3** was conducted and the outer diameter profile (O.D.) and inner diameter profile (I.D.) are shown in **Fig. 6**. We can observe that the deposited sphere was relative open in both end (60 mm diameter on the bottom and the top). Shrink is observed in the middle (or the equator 200 mm diameter), the same trend as in **Fig. 5**. This could be affected by the cooling after the WAAM process, since more material is deposited around 200 mm diameter, compared with both ends. From **Fig. 6**, we can also observe that the profile error is around 5 mm. Notice that the error bar shows the standard deviation (1σ) of the dimensions around Z-axis.

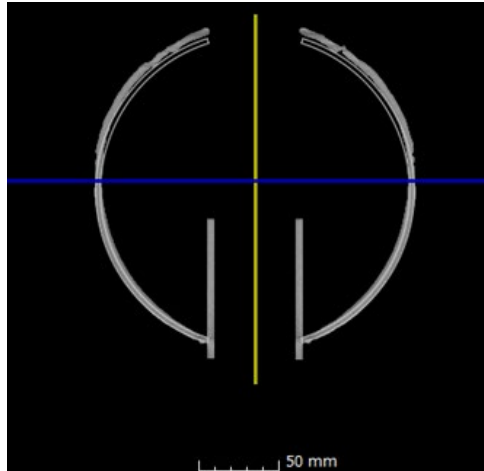


Fig. 5. Cross section of the deposited sphere measured by CT scanning

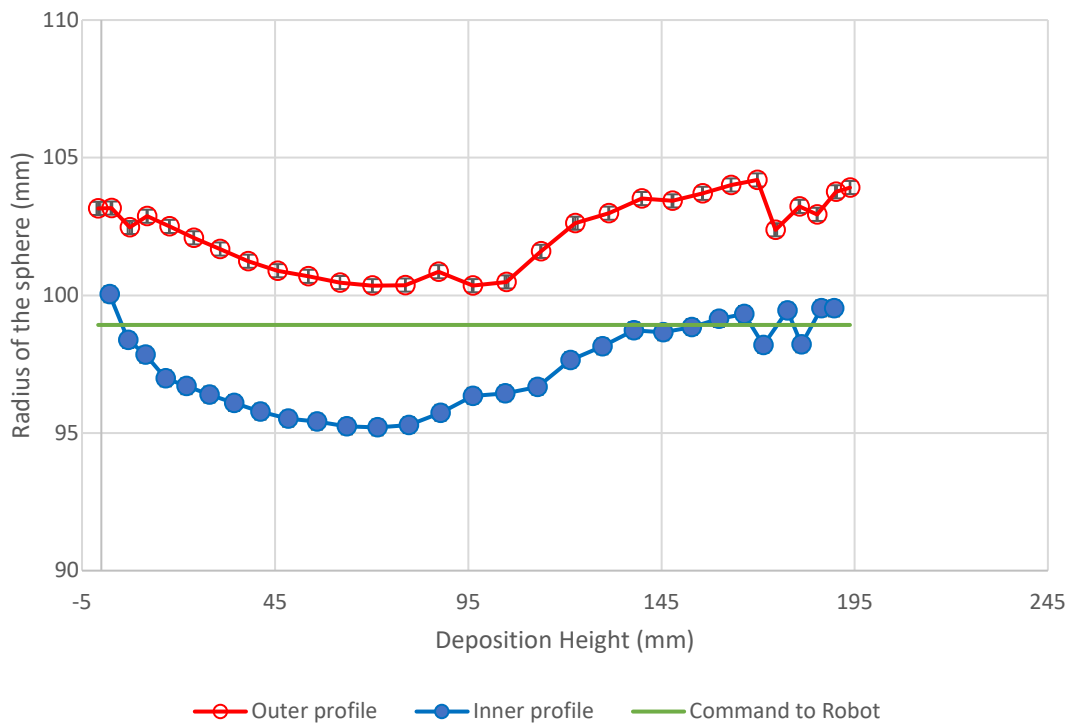


Fig. 6. The profile analysis of the deposited sphere depending on the deposition height

3. Wall thickness analysis

The wall thickness, which is mentioned as the weld bead width in [2], is shown in **Fig. 7**. The thickness varies depending on the deposition height sharply, especially in the beginning, the middle, and the end of the deposition. The thermal effect and the pose error of the robot, or even the gravity effect on the melting pool, could be the critical factors. However, the mechanism needs to be clarified in the next step research.

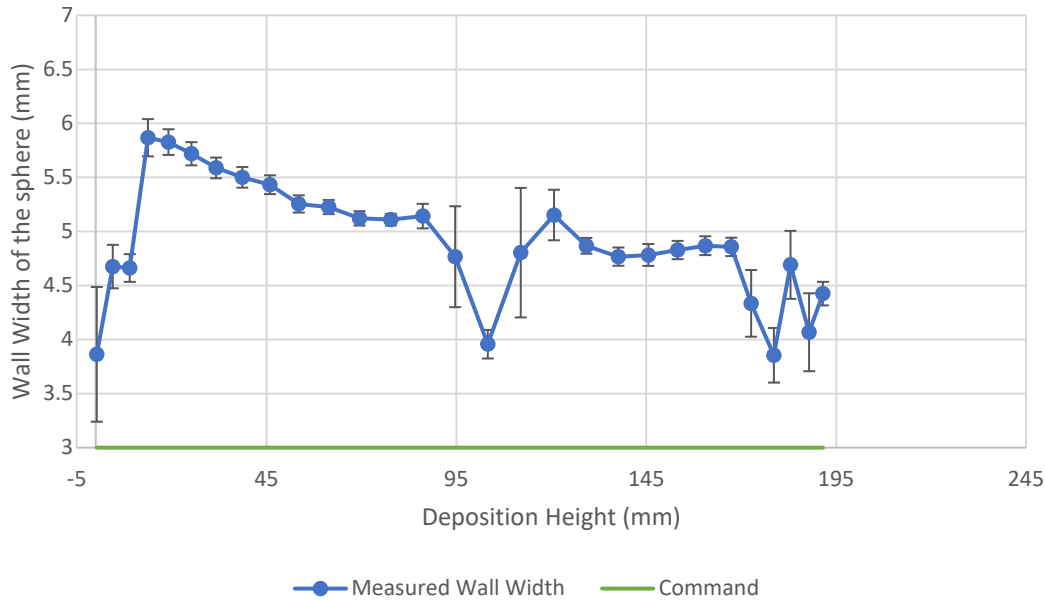


Fig. 7. The wall thickness of the deposited sphere depending on the deposition height

Conclusion and Discussion

This paper proposed a spherical test artifact and its quality evaluation process, for testing the geometric capability of the WAAM equipment. A mechanical configuration and the deposition strategy for depositing the proposed spherical shell shape was also considered. Since the mentioned WAAM system owns the potential to universally applying to large scale parts deposition, the authors will focus on the system design, software deployment and feedback system development of the proposed deposition strategy in the next stage.

Moreover, from the case study demonstrated in this study, the following research direction would be of interest in academia and needs further research efforts from the authors' understanding.

- The measurement and the improvement of both profile accuracy and the wall thickness stability.
- The influence of the error factors from WAAM equipment on the form accuracy.
- The non-destructive testing methods to replace CT scanning, especially for large scale parts.

References

- [1] S. W. Williams, F. Martina, A. C. Addison, J. Ding, G. Pardal, and P. Colegrove, "Wire + Arc Additive Manufacturing," *Materials Science and Technology*, vol. 32, no. 7, pp. 641–647, May 2016, doi: 10.1179/1743284715Y.0000000073.
- [2] T. Abe, J. Kaneko, and H. Sasahara, "Thermal sensing and heat input control for thin-walled structure building based on numerical simulation for wire and arc additive manufacturing," *Additive Manufacturing*, vol. 35, p. 101357, Oct. 2020, doi: 10.1016/j.addma.2020.101357.
- [3] P. Urhal, A. Weightman, C. Diver, and P. Bartolo, "Robot assisted additive manufacturing: A review," *Robotics and Computer-Integrated Manufacturing*, vol. 59, pp. 335–345, Oct. 2019, doi: 10.1016/j.rcim.2019.05.005.

- [4] M. K. Thompson *et al.*, “Design for Additive Manufacturing: Trends, opportunities, considerations, and constraints,” *CIRP Annals*, vol. 65, no. 2, pp. 737–760, Jan. 2016, doi: 10.1016/j.cirp.2016.05.004.
- [5] C. Buchanan and L. Gardner, “Metal 3D printing in construction: A review of methods, research, applications, opportunities and challenges,” *Engineering Structures*, vol. 180, pp. 332–348, Feb. 2019, doi: 10.1016/j.engstruct.2018.11.045.
- [6] O. Diegel, A. Nordin, and D. Motte, *A practical Guide to Design for Additive Manufacturing*. in Springer Series in Advanced Manufacturing. Springer, 2020.
- [7] “ISO/ASTM 52902:2019,” *ISO*. <https://www.iso.org/standard/67287.html> (accessed Apr. 25, 2023).
- [8] “ASTM-52922 | Guide for Additive Manufacturing -Design- Directed Energy Deposition.”
- [9] “Titanium pressure vessel for space exploration built successfully using the Wire + Arc Additive Manufacturing process,” *Cranfield Univerity*, Mar. 01, 2019. [Online]. Available: <https://www.cranfield.ac.uk/press/news-2019/titanium-pressure-vessel-for-space-exploration-built-successfully-using-the-waam-process#>
- [10] Y. Zhao, Y. Jia, S. Chen, J. Shi, and F. Li, “Process planning strategy for wire-arc additive manufacturing: Thermal behavior considerations,” *Additive Manufacturing*, vol. 32, p. 100935, Mar. 2020, doi: 10.1016/j.addma.2019.100935.
- [11] “World’s largest 3D printers,” *Relativity Space*. [Online]. Available: <https://www.relativityspace.com/stargate>
- [12] “Nonplanar 3D Printing of Bifurcating Forms | 3D Printing and Additive Manufacturing.” <https://www.liebertpub.com/doi/10.1089/3dp.2021.0023> (accessed Jun. 27, 2022).
- [13] T. Abe and H. Sasahara, “Layer geometry control for the fabrication of lattice structures by wire and arc additive manufacturing,” *Additive Manufacturing*, vol. 28, pp. 639–648, Aug. 2019, doi: 10.1016/j.addma.2019.06.010.
- [14] “Sapphire.” <https://velo3d.com/products/#sapphire>
- [15] “ISO/ASTM 52900:2021,” *ISO*. <https://www.iso.org/standard/74514.html> (accessed Apr. 25, 2023).
- [16] L. Nguyen, J. Buhl, R. Israr, and M. Bambach, “Analysis and compensation of shrinkage and distortion in wire-arc additive manufacturing of thin-walled curved hollow sections,” *Additive Manufacturing*, vol. 47, p. 102365, Nov. 2021, doi: 10.1016/j.addma.2021.102365.
- [17] S. Ibaraki and R. Usui, “A novel error mapping of bi-directional angular positioning deviation of rotary axes in a SCARA-type robot by ‘open-loop’ tracking interferometer measurement,” *Precision Engineering*, vol. 74, pp. 60–68, Mar. 2022, doi: 10.1016/j.precisioneng.2021.11.002.
- [18] *Welding work*, 5th edition., vol. IV. in Welding management of aluminum alloy structures, vol. IV. General Incorporated Association Light Metal Welding Association, 2020.
- [19] T. Zikmund *et al.*, “Computed tomography based procedure for reproducible porosity measurement of additive manufactured samples,” *NDT & E International*, vol. 103, pp. 111–118, Apr. 2019, doi: 10.1016/j.ndteint.2019.02.008.
- [20] “XT H 225,” *Nikon Industrial Metrology - Japanese*. <https://industry.nikon.com/ja-jp/products/x-ray-ct/xt-h-225-xt-h-320/> (accessed Apr. 27, 2023).
- [21] “VGSTUDIO,” *volumegraphics.com*. <https://www.volumegraphics.com/jp/products/vgstudio.html> (accessed May 09, 2023).
- [22] “Geomagic Wrap Software.” <https://oqton.com/geomagic-wrap/?smtNoRedir=1> (accessed Apr. 27, 2023).